Novel pressurised gyration device for making core-sheath polymer fibres

S. Mahalingam, S. Homer-Vanniasinkam, M. Edirisinghe *

Department of Mechanical Engineering, University College London, London WC1E 7JE, UK

HIGHLIGHTS

- Core-sheath polymer fibres are formed in a novel way.
- A new twin-reservoir device has been designed and constructed to enable this.
- The device was subjected to pressurised gyration.
- Microstructural characterisation confirms core-sheath fibre formation.
- Nanoparticles have been successfully incorporated in the product.

GRAPHICAL ABSTRACT
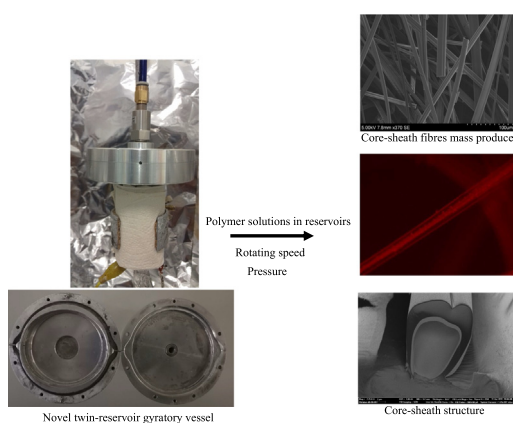
ABSTRACT

Core-sheath fibres of two polymers were generated using a novel set-up where rotating speed and pressure can be varied at ambient temperature. The specially designed spinneret consists of inner and outer chambers which can accommodate two polymers and other additives. The new methodology was demonstrated using poly(ethylene oxide) and poly(methylmethacrylate) (PMMA). Dyes were used as colouring agents for the polymers to verify core-sheath formation, and optical, scanning and fluorescent microscopy of the formed fibres confirmed the presence of a core-sheath combination. The core diameter obtained was in the range 5–10 μm and the sheath fibre diameter was 20–30 μm. The core/sheath diameter can be pre-set by selecting the forming conditions. To show the flexibility of the new method, nanoparticle containing PMMA fibres were also produced using the new device and incorporation of the nanoparticles in the sheath and core of the fibres was verified by electron microscopy and energy-dispersive X-ray spectroscopy analysis. A high yield of fibre was obtained and with more severe forming conditions the size of core-sheath fibres generated can be reduced to the nanoscale. Thus, the new process has a real capability of manufacturing a wide variety of novel functional materials and structures in a single scalable set-up.

1. Introduction

Core-sheath polymer fibres are an interesting class of materials and have received substantial attention due to its multitude of applications in areas such as solar and electrical, in food, drug delivery and tissue

* Corresponding author.
 E-mail address: m.edirisinghe@ucl.ac.uk (M. Edirisinghe).

engineering [1–9]. The extra phase in these fibres can have an unique characteristic compared to their single-phase counterparts. The core-sheath fibre has regular microstructure and a clear heterointerface [10]. In addition, it endows a material with a fascinating interfacial property. For example, developing tissue engineering scaffolds consisting of bi-phase core-sheath fibres are useful for integrative osteochondral repair. The micro-environments for bone and cartilage are different, therefore development of two-phase fibrous scaffolds show excellent biocompatibility and resemblance in structure to the natural extra cellular matrix of their respective tissues [11]. Core-sheath fibres have been also used in wound dressing and healing where these scaffolds possess more homogeneity, oxygen penetration and prevent infections and dehydration [12]. Similarly, development of core-sheath fibres containing two different phases could be exploited in bi-phasic drug release [13]. Generally, in biphasic drug release, active pharmaceutical ingredients are released at two different rates or periods and often an immediate release followed by a sustained release is ideal for delivering a wide variety of therapeutic ingredients such as non-steroidal anti-inflammatory drugs, anti-allergic and antihistaminic agents. Core-sheath structures showed excellent drug release characteristics and had sustained drug release compared to blended fibres [14]. In addition, core-sheath fibres were shown to induce excellent strength in fibres, a property still a major challenge in single-phase fibres [10].

Pressurised gyration is a simple and versatile ambient temperature technique to mass produce fibres and fibrous structures with controllable fibre size and fibre size distribution with high yield [15]. The technique consists of a vessel containing polymer solution subjected to simultaneous centrifugal force and dynamic fluid flow to extrude fibres with tailored morphologies and functionality. The fibres produced by this technique depend on rotating speed of the vessel, air pressure and the concentration of polymer solution. Indeed, unlike electrospinning it is a nozzle free method independent of electrical conductivity and dielectric constant of polymer solution. The process also offers production of fine long continuous anisotropic fibres. Fibres with high molecular orientation can provide mechanically stronger fibres with remarkable surface-active areas. Over the last five years pressurised gyration has gone through many developments to process a wide variety of advanced functional materials and structures [16]. Process variations, such as infusion gyration is capable of producing protein tagged fibres by controlling the flow of polymer solution rather than pressure [17]. Likewise, pressure-coupled infuse gyration where flow rate of material into the rotating vessel is controlled simultaneously with pressure has been shown to form well aligned nanofibres with excellent size control [18]. However, more dramatic modifications in pressurised gyration are needed to process core-sheath fibres through development of an innovative spinneret.

In this work, we report, the creation of core-sheath polymer fibres generated by pressurised gyration. To achieve this breakthrough, we designed a new spinneret, which is the first of a series of devices we intend to create. It consists of inner and outer reservoirs which can accommodate two different polymer solutions to generate core-sheath structures. This first attempt is also shown to be useful for the encapsulation of other constituents e.g. nanoparticles in the resultant microstructures.

2. Experimental

2.1. Materials

Aluminium metal (Grade - BS EN755 6082-T6) was used to make the spinneret, the design and construction of which is explained further in section 2.3. Poly (ethylene oxide) (PEO) ($M_w = 200,000$ gmol^{-1}), Poly(methylmethacrylate) (PMMA) ($M_w = 120,000$ gmol^{-1}) and red colour Sudan IV (Dye content, 80%) were obtained from Sigma Aldrich, UK, the latter was used to colour PMMA. Red colour food dye was obtained from a local trade station for use as a dye for PEO. Only one dye

was used at a time, to indicate the core of the core-shell fibre. De-ionised water and chloroform were used as the solvents for PEO and PMMA, respectively. The two polymers were chosen because one is water soluble (PEO) and the other is non-water-soluble polymer (PMMA). Thus, they are not miscible polymer solutions and phase separation could be easily obtained. Another reason is that we have used water as a solvent for PEO and chloroform as a solvent for PMMA. The boiling point of water is higher than the boiling point of chloroform. Therefore, the solidification of PMMA fibres is easily obtained when used as inner and outer capillary solutions. Ag-Cu-W composite nanoparticles in chloroform were obtained from University of Hertfordshire and their details are published elsewhere [16].

2.2. Solution preparation and characterisation

15 wt% (w/w) PEO was dissolved in de-ionised water and magnetically stirred for 24 h at ambient temperature (~20 °C). 15 wt% (w/w) PMMA was dissolved in chloroform and magnetically stirred for 24 h at ~20 °C. Then 1 ml of Sudan dye was mixed with PMMA solution and stirred for 2 h prior to pressurised gyration. Likewise, 1 ml of food dye was mixed with PEO solution prior to pressurised gyration. The solutions with dyes were used specifically for core fibre formation in this work.

The surface tension and viscosity of the 15 wt% PEO and 15 wt% PMMA polymer solutions were characterised using calibrated Kruss Tensiometer and Brookfield Viscosity-meter, respectively. For 15 wt% PEO polymer solution the surface tension was 52 mN/m and the viscosity was 2200 mPa s. For 15 wt% PMMA polymer solution the surface tension was 41 mN/m and the viscosity was 171 mPa s.

2.3. Spinneret design and fabrication

Fig. 1a shows the design of the core-sheath pressurised gyration device. There are two aluminium cylindrical vessels embedded together. The diameter of outer vessel is 100 mm and the inner vessel is 80 mm. In the middle of the alignment there is an opening for the pressurised gas connection. The opening has a dimension of 15 mm outer diameter and the 6 mm inner diameter. The thickness of the outer vessel is 20 mm and the inner vessel is 10 mm. In addition, there are two protruding capillaries connected to vessels. The dimensions of the capillaries were 1.6 mm outer diameter and 0.8 mm inner diameter. The device was designed in such a way that upper and lower die halves could be assembled using bolts. The materials to processed (e.g. polymer solution) are placed in the lower die moulds in appropriate quantities. The vessel is connected to a DC motor at the bottom through a screw-joint.

The two halves of the device and the assembled device used at ambient conditions (20 °C, relative humidity 42%) in this study are shown in Fig. 1b, c and d. One end of the vessel was connected to a motor which can generate apparent speeds up to 6000 rpm, while the other end was connected to a nitrogen gas stream, the pressure of which can be varied up to 3×10^5 Pa. Speed of the gyration vessel was calibrated by attaching a photo-sensitive tape to face of the vessel and with a tachometer. To facilitate the collection of fibres a stationary collector made of aluminium foil was placed around the spinning vessel.

2.4. Core-sheath fibre preparation

5 ml of PEO and PMMA solutions were used as core material in separate experiments. 4 ml PEO and PMMA solutions were used as sheath fibre material in corresponding experiments. In each case fibres were spun at 6000 rpm and 0.1 MPa pressure. The spinneret was operated for 60s in each case. The process of core-sheath fibre formation was
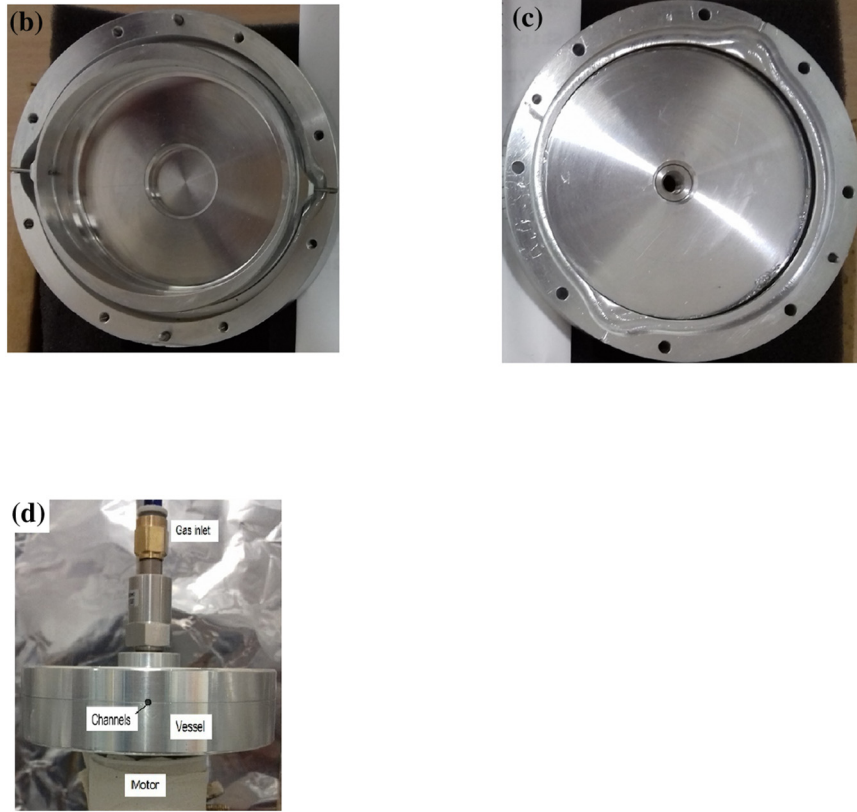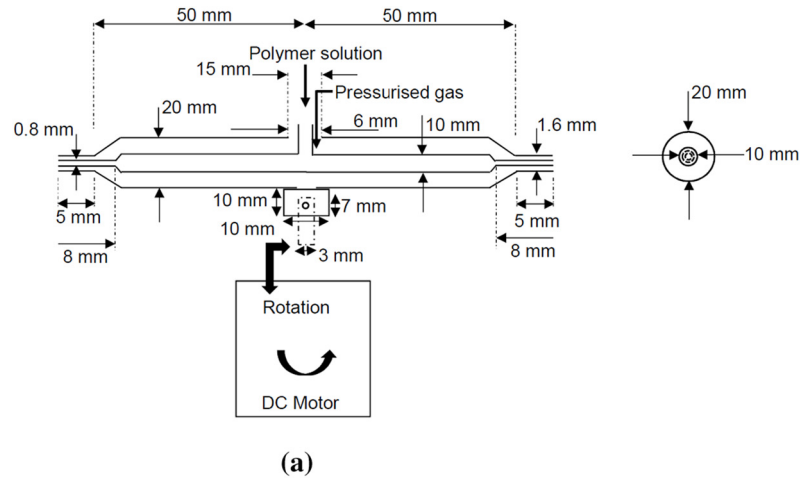
Fig. 1. (a) Design features of spinneret device. Interior view of new device (b) Bottom half (c) Top half (d) Experimental set-up.

captured using a high-speed camera capable of recording 10,000 frames per second (see Supplementary information for Video illustrating the new process). Table 1 shows the polymer systems that were used in this work.

2.5. Encapsulation of nanoparticles in PMMA fibres

Encapsulation of Ag-Cu-W nanoparticles was also attempted as follows: 5 ml of nanoparticle solution (in chloroform) was loaded in the

Table 1
Polymer systems and the corresponding sample numbers. Volume refers to amount of solution in spinning device.

Sample	Core				Sheath	
	Polymer (wt%)	Spinning time (s)	Dye (wt%)	Volume (ml)	Polymer (wt%)	Volume (ml)
1	PEO (15)	60	Food (0.5)	1–5	PMMA (15)	1–4
2	PMMA (15)	30	Sudan IV (0.5)	1–5	PEO (15)	1–4
3	PMMA (15)	30	Sudan IV (0.5)	1–5	PMMA (15)	1–4
4	PEO (15)	60	Food (0.5)	1–5	PEO (15)	1–4

inner reservoir of the vessel and 5 ml of PMMA solution was loaded in the outer reservoir. They were simultaneously spun at 6000 rpm and 0.1 MPa pressure.

2.6. Microstructural characterisation

Core-sheath samples deposited in the aluminium foil were collected using glass microscope slides. These were sealed in a petri-dish and maintained at the ambient temperature. The samples were observed using a Nikon Eclipse ME600 optical microscope. The fibres were also characterised using a fluorescence microscope (EVOS FL, Life Technologies) to verify the core-sheath fibre formation in each case.

The nanoparticle containing PMMA fibres were studied using field emission scanning electron microscopy (FE-SEM, model JSM 6301 F). Before imaging, samples were coated with carbon using a Edwards Sputter S1 50B coater for 75 s. Energy dispersive X-ray analysis was performed to verify the nanoparticle incorporation. Focused ion beam milling and imaging was performed on samples to verify the core-sheath structure using a Zeiss NV40 FIB/SEM machine. The milling and polishing of the sample have been done with a current of 150 pA and 80 pA, respectively. The images were obtained at 5 kV applied voltage.

3. Results and discussion

3.1. Core-sheath fibre formation

The formation of core-sheath fibres using this technique could be explained by Rayleigh-Taylor instability at the liquid-air interface. The external driving force is the centrifugal force that acts in the direction away from the centre of the gyration vessel when the polymer solution emerges from the respective channels. The surface tension force will oppose this centrifugal force in the opposite direction to withhold the materials in the channels. In addition to this centrifugal force there is a dynamic fluid flow force originating from the blowing action of gas in the channels. This results in elongation of polymer liquid jets in the channels. The polymer solution and the air have dissimilar densities. This will generate perturbation in the polymer liquid jet. The liquid jet will be pushed upwards and downwards continuously during spinning. When the maximum wavelength of the polymer liquid jet is reached then it will be detached from the main stream to form polymer fibres. Finally, the evaporation of solvents leads to thinning of the fibres formed. The formation of the core and sheath fibres must happen at the same time to have core-sheath structure. Otherwise, fibres will be formed individually from the respective channels resulting in single material fibre structures as in our previous work [16]. To ensure core-sheath fibre structure formation, flow synchronisation is essential. Hence, sheath fibre formation was tested individually (one reservoir loaded) given its flow is the limiting factor due to higher centrifugal force and the low loading capacity. By increasing the volume of polymer solution and finding out the respective yield for each case, an idealised volume is derived and its time taken to form the fibres was evaluated. Based on this the core flow is manipulated to achieve synchronisation. Essentially there are three steps involved in forming of the core-sheath structure. (i) polymer solutions were driven by centrifugal force in opposition to withholding capillary force (ii) pressurised gas stretches the fibre in the spinning direction (iii) solvent evaporates and solidification of fibre takes place.

To study the effect of rotating speed on core-sheath fibre formation PEO polymer solution is loaded in the inner vessel and PMMA solution is loaded in the outer vessel. The solutions were spun at 2000 rpm rotating speed and 0.1 MPa working pressure. There was no output. The rotating speed was gradually increased to 4000 rpm while the working pressure was kept constant. In this scenario also, there were no materials formed. Finally, the rotating speed was increased to 6000 rpm and working pressure was kept at 0.1 MPa. This combination of rotating speed and the

working pressure yielded the core-sheath structures and they are presented below.

3.2. PEO core and PMMA sheath fibres

Fig. 2a shows optical micrographs of the PEO core – PMMA sheath fibres. The depth of field is fine tuned to indicate the core-sheath fibre formation. The brighter region corresponds to the core of the fibre and the darker region corresponds to the sheath. Fig. 2b shows a fluorescence micrograph of the fibre, the bright red colour (highlighted with dotted line) shows the core of the fibre. Both micrographs illustrate the core-sheath fibres with an equidistant central core region running across the fibre length.

3.3. PMMA core and PEO sheath fibres

Fig. 2c shows the optical micrographs of the PMMA core and PEO sheath fibres. The brighter region corresponds to the PMMA core and the darker region corresponds to the PEO sheath. Fig. 2d shows fluorescence micrographs of the PMMA core and PEO sheath. It was also observed that swapping the solvent systems shows the formation of beads in the core while the sheath remains uniform and smooth.

3.4. PEO core and PEO sheath fibres

In this scenario, fibres failed to form due to much lower evaporation of the solvent from inner and outer capillaries during the jetting process. Water has a higher boiling point (~100 °C) compared to chloroform (~61 °C) used with PMMA, therefore it will take longer to evaporate completely at ambient temperature. Since the inner and outer vessels consists the same phase during spinning, the jets ejected from the capillaries remained in liquid state preventing formation of solid fibres.

3.5. PMMA core and PMMA sheath fibres

Optical microscopy illustrates the dyed core as a lighter shade of material with varying cross section running along the fibre length (Fig. 2e). This result is verified in the fluorescence micrograph shown in Fig. 2f, dotted line highlighting the core.

3.6. Core-sheath fibre diameter distribution

Fig. 3a–f shows the fibre diameter distribution for different polymer systems. One hundred fibres were used for analysis. In the PEO core – PMMA sheath polymer system, the mean core diameter is 6.7 ± 1.1 μm (Fig. 3a). The mean sheath diameter is 20.5 ± 1.4 μm (Fig. 3b). The polydispersity index of the distribution for these two cases is ~16% and ~7%, respectively. Similarly, for the PMMA core – PEO sheath polymer scenario, the mean core diameter is 8.5 ± 3.3 μm (Fig. 3c), the mean sheath diameter is 24.8 ± 0.6 μm (Fig. 3d) and the polydispersity index of the distribution for these two cases is ~39% and 2.5%, respectively. The mean core and sheath diameter are 5.8 ± 1.1 μm and 31.5 ± 0.6 μm, respectively, for the PMMA core – PMMA sheath polymer system (Fig. 3e, f), the polydispersity index of the distribution in each case is ~20% and ~2%, respectively. Fig. 4 shows analysis of the core-sheath fibre diameters obtained in this work. As expected, in all cases the mean core fibre diameter is less than the mean sheath fibre diameter. PMMA polymer showed the higher mean fibre diameter for core and sheath components when coupled with PEO.

Fig. 5 shows the scanning electron micrographs of the core-sheath fibres obtained in this process. In all cases the fibres appear as smooth and continuous. However, surface morphology, size and shapes of the fibres could be tailored to suite by changing the processing conditions and the orifice size and shape.

The variation in the fibre diameter and diameter distribution for the different polymer systems shows that tailoring of the fibre size and size
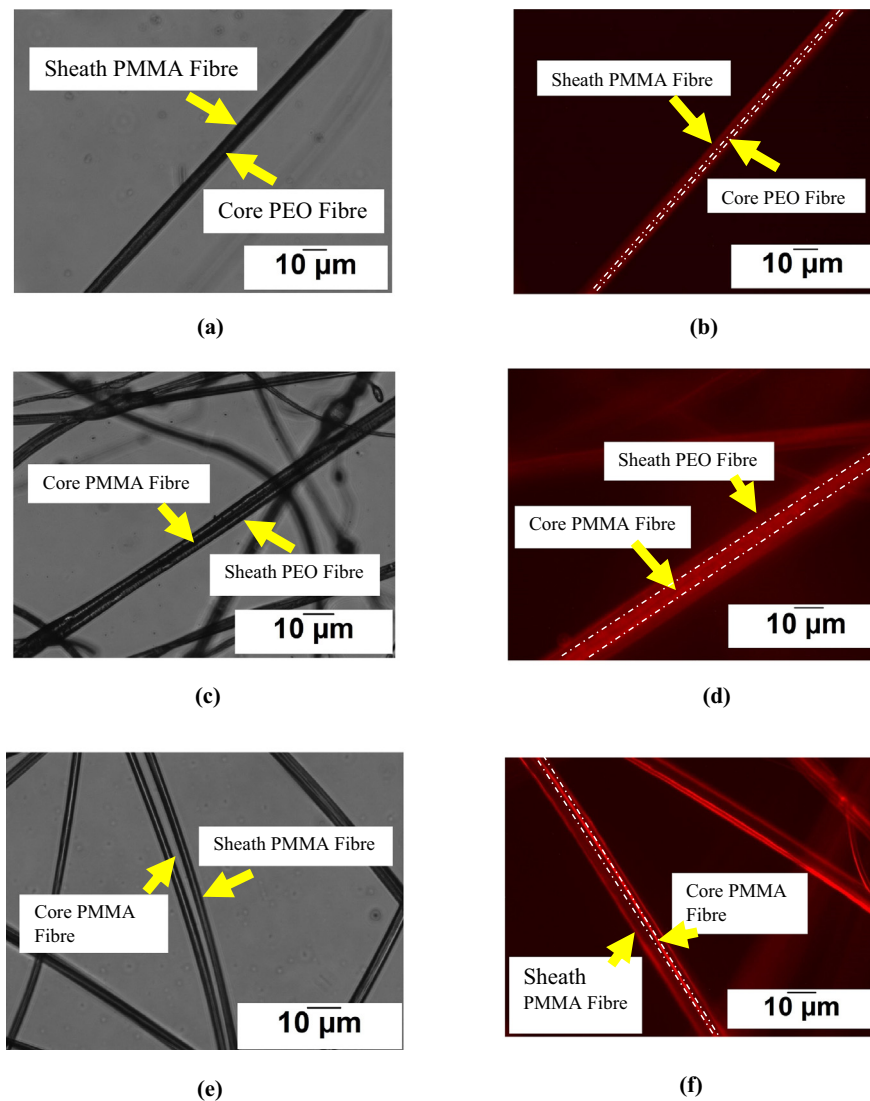
Fig. 2. (a) Optical and (b) fluorescence micrographs showing core-sheath fibre formation in PEO core-PMMA sheath system, (c) Optical and (d) fluorescence micrographs showing core-sheath fibre formation in PMMA core-PEO sheath system. (e) Optical and (f) fluorescence micrographs of PMMA core - PMMA sheath fibres. Dark outer region indicative of PMMA sheath and the brighter inner region indicates PMMA core.

distribution is possible in this forming method. However, relevant optimization is necessary to avoid polymer bead formation. It is well known that polymer molecular weight and polymer chain entanglement significantly affect fibre morphologies. Fabricating continuous fibre morphologies require sufficient polymer entanglement, and for a given molecular weight, the entanglement density increases with concentration of the polymer and minimises 'bead on string' fibre morphology. The molecular weight determines the critical chain overlap concentration. Fibre morphologies are shown to be greatly affected by critical chain overlap concentration. Thus, as the polymer concentration increases, the overlapping of polymer chains form sufficient entanglement networks of polymer chains. Bead-free continuous fibres are formed when the polymer concentration is above the critical concentration. However, increasing the concentration of the polymer increases the viscosity of polymer solution hindering solvent evaporation, and this results in thicker fibres or solidification takes place during spinning and fibres cannot be formed. If the concentration of polymer is too low, only droplets or beads were formed or the creation of bead on string fibres were promoted. By optimising polymer concentration and using higher pressures like in single material gyration [15] finer core-sheath fibres on a nanoscale may be prepared.

3.7. Nanoparticles in fibres

Fig. 6 shows nanoparticle containing PMMA fibres formed in this process. The white spots on the fibres are verified as Ag-Cu-W nanoparticles using energy dispersive X-ray analysis. A striking observation is that nanoparticles are quite well evenly distributed on the fibre surface. Even though the nanoparticles solution was contained within the inner chamber which generates the fibre core, the particles appeared on the outer surface of the fibres. This shows, there is a simultaneous solution spraying and spinning of two different solutions occurring during forming. The outer chamber provides the polymer solution which is drawn out as polymer jets from its outlet. Since the polymer solution has sufficient polymer chain entanglement and viscosity the fibres are extruded from the outlet. However, the inner chamber contains nanoparticle solution lacking polymer chain entanglement and viscosity. Therefore, this outlet draws out the liquid jet (in this case solvent chloroform) which breaks up as tiny droplets containing nanoparticles. These nanoparticle containing droplets will land on the polymer liquid jets during forming. Finally, the droplet evaporates and leaves the nanoparticles on the polymer fibres. The nanoparticle containing core-sheath fibres could be used as face masks, air-water filtration mats and tissue
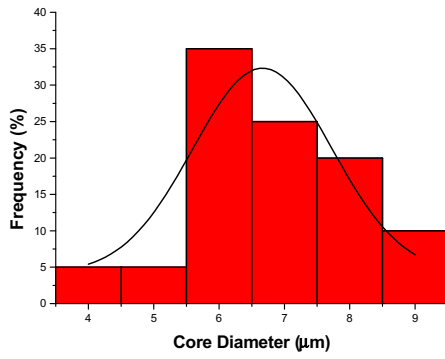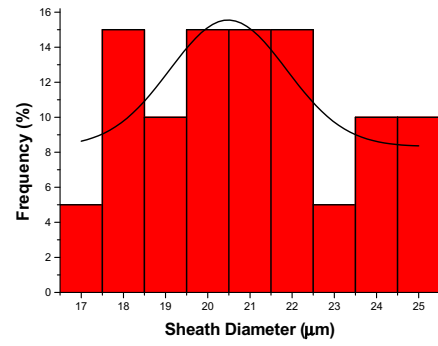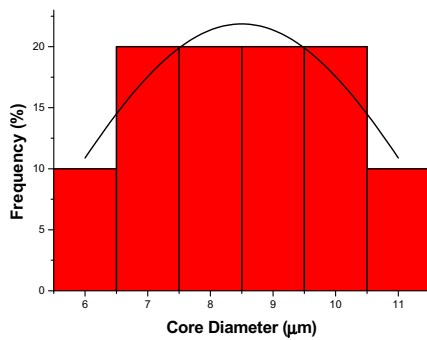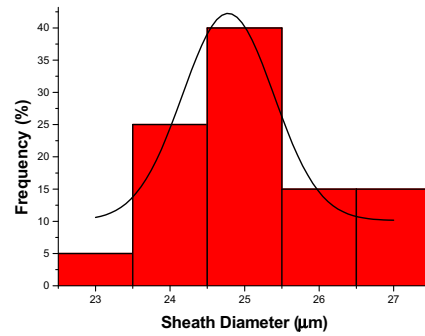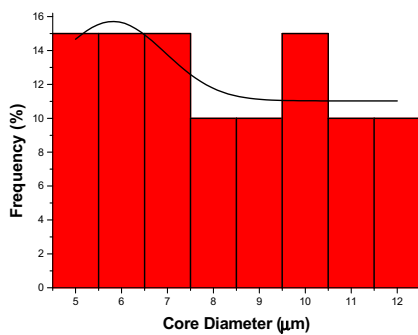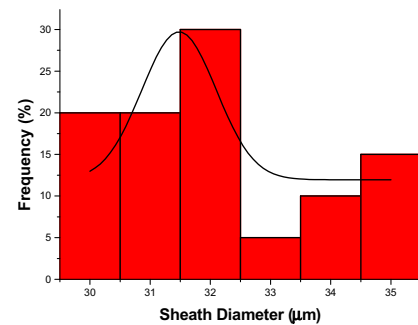
Fig. 3. (a)–(f) Fibre diameter distribution of the core-sheath fibres for various polymer systems: (a), (b) Core, Sheath fibre diameters of PEO-PMMA fibres (c), (d) Core, Sheath fibre diameters of PMMA-PEO fibres (e), (f) Core, Sheath fibre diameters of PMMA-PMMA fibres.

engineering scaffolds. The function of the nanoparticle is to scavenge the microorganism that is coming into contact with the fibrous structures. The fibrous structures can be used to protect environmental hazards (face mask), filter out the particles (e.g. CaCO₃) and other impurities (air-water filters). In tissue engineering these are used to mimic the extra cellular matrix of the biological bodies where cells are attached and grown under suitable conditions to generate a new tissue or organ or replace damaged or burnt tissues. The nanoparticles will inhibit any microorganisms (e.g. bacteria) during the tissue regeneration process and facilitate the smooth functioning of the scaffolds.
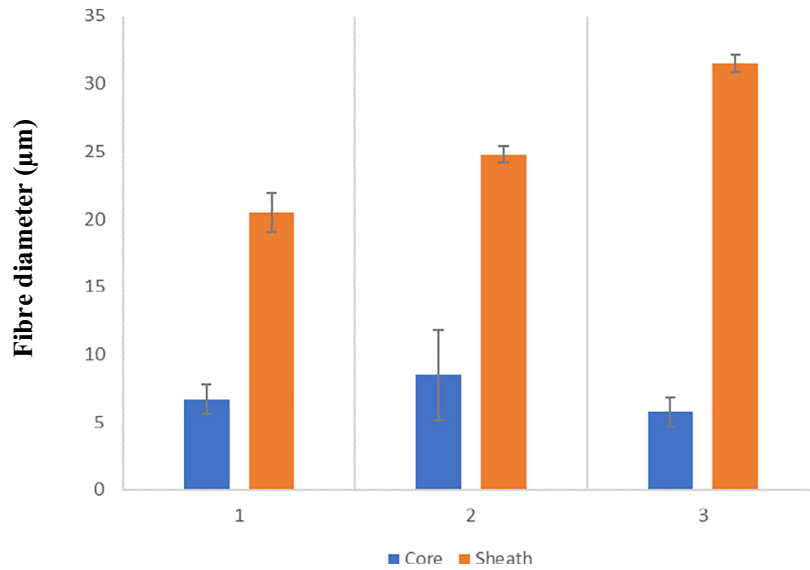
Fig. 4. Analysis of the core-sheath fibre diameters obtained in this work (1) PEO-PMMA fibres (2) PMMA-PEO fibres (3) PMMA-PMMA fibres.

3.8. Focussed ion beam imaging and scanning electron micrograph

Fig. 7(a) and (b) show the scanning electron micrograph of core-sheath fibre before and after ion milling. Fig. 7(a) shows the fibre as a single fibre and there is no clear evidence the core-sheath structure has been formed. However, the Fig. 7(b) reveals there are two phases existing within the fibre. A sharp contrast change within the fibres indicates that core-sheath fibre has been obtained. The darker region corresponds to the core of the fibre while the brighter region corresponds to the sheath of the fibre. Fig. 7(c) shows the backscattered electron imaging of the core-sheath fibre. It is clearly seen there are nanoparticles located within the fibre and the fibre surface. This demonstrates that this manufacturing method is very effective for incorporating the nanoparticles.

3.9. Yield of the fibres

The yield of this method is compared with other well-established techniques and shown in Table 2 below. The new core-sheath pressurised gyration technique provides higher yield than the
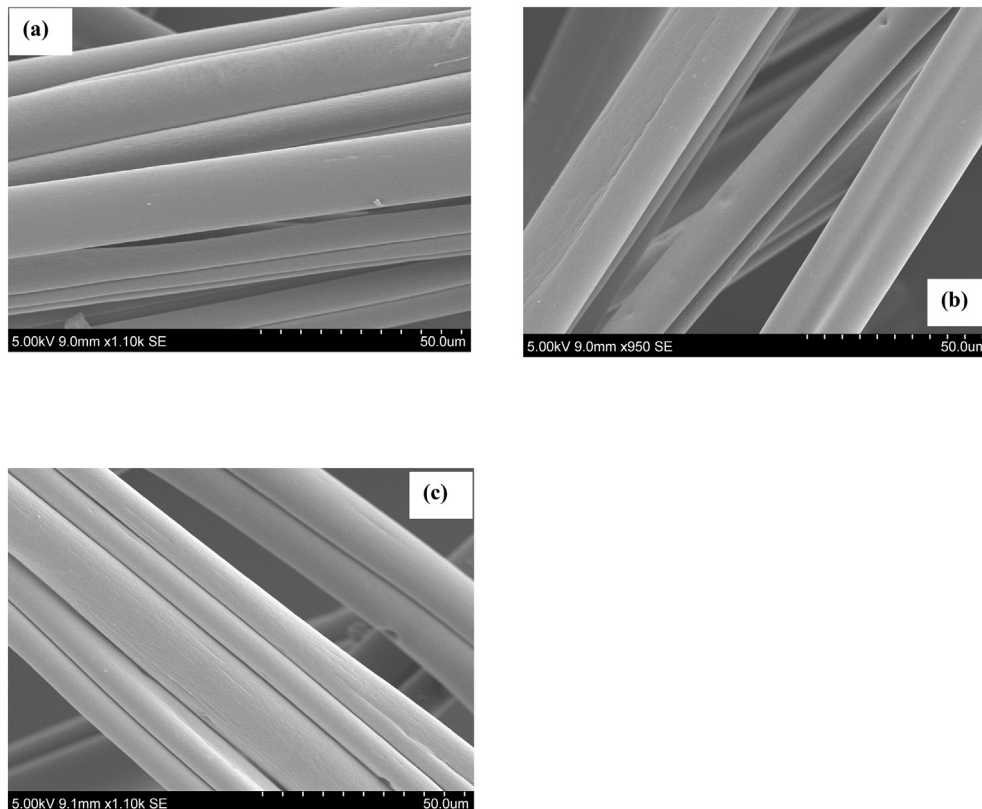

Fig. 5. Scanning electron micrographs showing the surfaces of the core-sheath fibres (a) PEO-PMMA (b) PMMA-PEO (c) PMMA-PMMA.
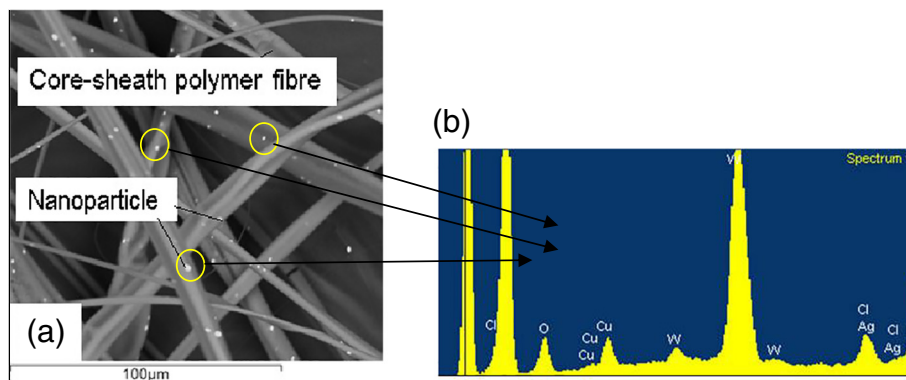
Fig. 6. (a) Nanoparticle containing PMMA fibres (b) EDX analysis on the nanoparticles confirmed existence of Ag/Cu/W elements.

centrifugal spinning and electrospinning methods. The yield is two orders and an order of magnitude higher than the centrifugal spinning and electrospinning, respectively. The yield is less than the value we reported in our earlier work for single material pressurised gyration. This is due to the different surface tension and viscosity of polymer systems used in this work and the different lower rotating speed of the spinning systems. The rotating speed of core-sheath twin reservoir gyration device is lower than the single reservoir pressurised gyration as its architecture is very different. In addition, the latter spinneret design contained 20 orifices to deliver output, compared with two orifices used in the present work. Also, the volume of materials delivered to the output channel is much lower in the present work compared to previous work [15] as the current spinneret makes 100 revolutions in a second compared to 600 in previous work [15]. Core-sheath fibre size obtained in this work is in the micrometre range however size of the fibres generated in electrospinning ranges from micro-nano range. Modification of the outlet sizes (both inner and outer) to lower than existing sizes used in the present work and the application of pressure >0.1 MPa (atmospheric) have produced core-sheath fibres in the nanometer scale and is being further investigated at present. With respect to morphology of the fibres, all the core-sheath fibres obtained from all the techniques (pressurised gyration, electrospinning and centrifugal spinning) show smooth, continuous fibre morphology. However, these techniques including pressurised gyration could be used to tailor the desired morphology by adjusting the process parameters and the outlet size and shape.

4. Conclusions

A novel pressurised gyration-based device and manufacturing route have been developed to generate core-sheath fibres in a single step. Sufficient evidence was gained to conclude core-sheath fibre formation in different polymeric systems. Encapsulation of nanoparticles in fibres was verified by energy dispersive x-ray analysis. This indicates that the new design and methodology will pave the way to make various novel functional materials and structures and this will be a very significant development especially for applications in energy and biomedical scenarios.

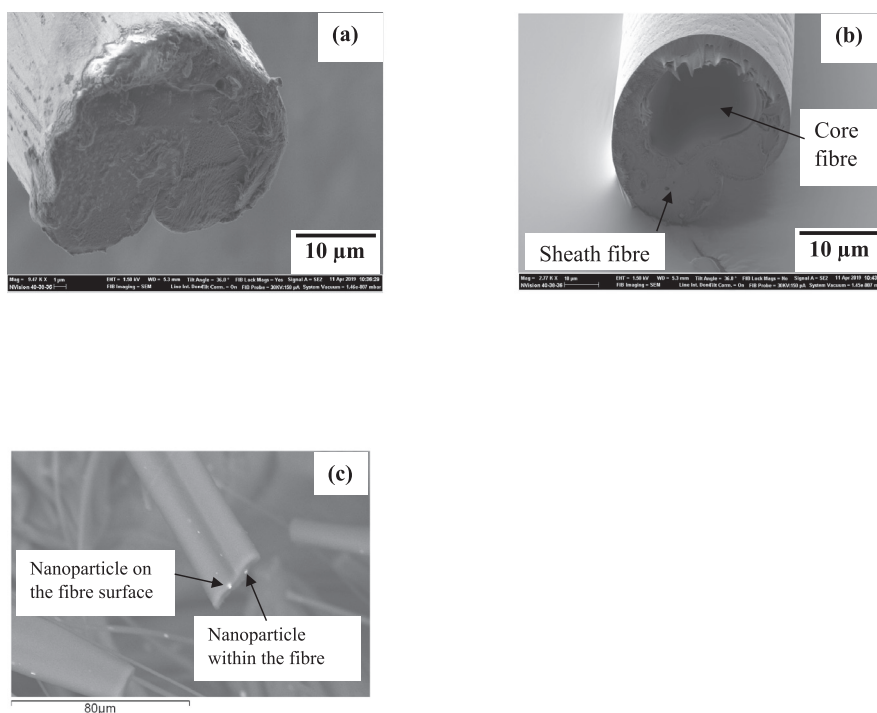Supplementary data to this article can be found online at https://doi.org/10.1016/j.matdes.2019.107846.

Fig. 7. Scanning electron micrographs of core-sheath fibres: (a) Before ion milling (b) After ion milling (c) Backscattered scanning electron microscope image shows nanoparticle within the fibre and nanoparticle on the fibre surface.

Table 2
Comparison of yield for different techniques.

Technique	Yield (kgh^{-1})
Centrifugal spinning [19]	0.06
Solution blowing [20]	7–8
Electrospinning [19]	0.17
Single material pressurised gyration [15]	6
Core-sheath pressurised gyration (this work)	3.2

CRediT authorship contribution statement

S. Mahalingam: Conceptualization, Data curation, Formal analysis, Funding acquisition, Investigation, Methodology, Writing - original draft, Writing - review & editing. **S. Homer-Vanniasinkam:** Conceptualization, Formal analysis, Funding acquisition, Investigation, Writing - original draft, Writing - review & editing. **M. Edirisinghe:** Conceptualization, Data curation, Formal analysis, Funding acquisition, Investigation, Methodology, Project administration, Writing - original draft, Writing - review & editing.

Acknowledgements

References

[1] G. Kwak, G.H. Lee, S.-H. Shim, K.B. Yoon, Fabrication of light-guiding core/sheath fibers by coaxial electrospinning, Macromol. Rapid Commun. 29 (10) (2008) 815–820.
[2] D.G. Yu, C. Branford-White, S.W.A. Bligh, K. White, N.P. Chatterton, L.M. Zhu, Improving polymer nanofiber quality using a modified co-axial electrospinning process, Macromol. Rapid Commun. 32 (9–10) (2011) 744–750.
[3] M. Wei, J. Lee, B.W. Kang, J. Mead, Preparation of core-sheath nanofibers from conducting polymer blends, Macromol. Rapid Commun. 26 (14) (2005) 1127–1132.
[4] M.C. Zhang, C.Y. Wang, Q. Wang, M.Q. Jian, Y.Y. Zhang, Sheath-core graphite/silk fiber made by dry-meyer-rod-coating for wearable strain sensors, ACS Appl. Mater. Interfaces 8 (32) (2016) 20894–20899.
[5] X.T. Li, T. Hua, B.G. Xu, Electromechanical properties of a yarn strain sensor with graphene-sheath/polyurethane-core, Carbon 118 (2017) 686–698.
[6] K.S. Kumar, I. Siva, N. Rajini, J.T.W. Jappes, S.C. Amico, Layering pattern effects on vibrational behavior of coconut sheath/banana fiber hybrid composites, Mater. Des. 90 (2016) 795–803.
[7] C.K. Liu, H.-J. He, R.-J. Sun, Y. Feng, Q.-S. Wang, Preparation of continuous nanofiber core-spun yarn by a novel covering method, Mater. Des. 112 (2016) 456–461.
[8] A.M. Xie, K. Zhang, M.X. Sun, Y.L. Xia, F. Wu, Facile growth of coaxial Ag@polypyrrole nanowires for highly tunable electromagnetic waves absorption, Mater. Des. 154 (2018) 192–202.
[9] R. Hufenus, L. Gottardo, A.A. Leal, A. Zemp, K. Heutschi, P. Schuetz, Melt-spun polymer fibers with liquid core exhibit enhanced mechanical damping, Mater. Des. 110 (2016) 685–692.
[10] R. Kemp, B. Klumperman, N.P. Gule, Novel core-sheath antimicrobial nanofibrous mats, J. Appl. Polym. Sci. 35 (22) (2018), 46303.
[11] T. Zhang, H.F. Zhang, L.Q. Zhang, S.J. Jia, J. Liu, Z. Xiong, W. Sun, Biomimetic design and fabrication of multilayered osteochondral scaffolds by low-temperature deposition manufacturing and thermal-induced phase-separation techniques, Biofabrication 9 (2) (2017), 025021.
[12] C.J. Wang, G.L. Meng, L.Q. Zhang, Z. Xiong, J. Liu, Physical properties and biocompatibility of a core-sheath structure composite scaffold for bone tissue engineering in vitro, J Biomed Biotechnol (2012), 579141. https://doi.org/10.1155/2012/579141.
[13] H. Yu, P. Yang, Y.T. Jia, Y.M. Zhang, Q.Y. Ye, S.M. Zeng, Regulation of biphasic drug release behavior by graphene oxide in polyvinyl pyrrolidone/poly(epsilon-caprolactone) core/sheath nanofiber mats, Colloids Surf. B 146 (2016) 63–69.
[14] Y.-N. Jiang, H.-Y. Mo, D.-G. Yu, Electrospun drug-loaded core-sheath PVP/zein nanofibers for biphasic drug release, Int. J. Pharm. 438 (1–2) (2012) 232–239.
[15] S. Mahalingam, M. Edirisinghe, Forming of polymer nanofibers by a pressurised gyration process, Macromol. Rapid Commun. 34 (14) (2013) 1134–1139.
[16] P.L. Heseltine, J. Ahmed, M. Edirisinghe, Developments in pressurized gyration for the mass production of polymeric fibers, Macromol. Mater. Eng. 303 (9) (2018), 1800218.
[17] S. Zhang, B.T. Karaca, S.K. VanOosten, E. Yuca, S. Mahalingam, M. Edirisinghe, C. Tamerler, Coupling infusion and gyration for the nanoscale assembly of functional polymer nanofibers integrated with genetically engineered proteins, Macromol. Rapid Commun. 36 (14) (2015) 1322–1328.
[18] X. Hong, S. Mahalingam, M. Edirisinghe, Simultaneous application of pressure-infusion-gyration to generate polymeric nanofibers, Macromol. Mater. Eng. 302 (6) (2017), 1600564.
[19] C.J. Luo, S.D. Stoyanov, E. Stride, E. Pelan, M. Edirisinghe, Electrospinning versus fibre production methods: from specifics to technological convergence, Chem. Soc. Rev. 41 (2012) 4708–4735.
[20] S.R. Malkan, An overview of spun-bonding and melt-blowing technologies, TAPPI J. 78 (1995) 185–190.